SECTION C4

LOCAL INSTABILITY

TABLE OF CONTENTS

* To be supplied

C4.0.0 LOCAL INSTABILITY

C4.1.0 Introduction

This section deals with local instabilities and failures of flat and curved panels. The term "panel" refers to a composite structure consisting of plates and stiffeners. The term "plate" refers to sheet or skin bounded by longitudinal and tranverse members (e.g., stiffeners and frames). Panels in compression are of primary importance in this section. Although panels in shear are discussed, information concerning them is not as extensive as that for panels in compression.

Stability analyses of panels should account for both general and local modes of instability. The general mode of instability for a compression-loaded panel is characterized by deflection of the stiffeners; whereas, for local instability, buckling occurs with modes along (or nearly along) the stiffener-plate juncture (Fig. C4.1.0-1). Some coupling between these modes exists, but this effect is usually small and is generally neglected.

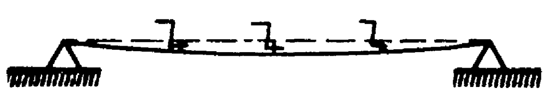

General Instability

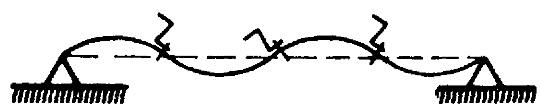

Local Instability

FIGURE C4.1.0-1. TYPICAL BUCKLE MODES IN LONGITUDINALLY STIFFENED PLATES UNDER LONGITUDINAL LOAD.

Definition of Symbols

Symbol	Definition
a	long-side dimension of a plate, in.
b	short-side dimension of a plate, in.
b'	short-side dimension of a rectangular tube, in.
b_f	width of stiffener flange, in.
b_o	geometric fastener offset, in.
b_s	stiffener spacing, in.
b_T	width of hat top for hat-section stiffeners, in.
b_w	depth of stiffener web, in.
d	fastener diameter, in.
d_f	frame spacing, in.
e	end-fixity coefficient
E	Young's modulus of elasticity, psi
E_s, E_t	secant and tangent moduli, psi
f	actual stress, psi; also effective fastener offset, in.
F	allowable or buckling stress, psi
$F_{0.7}$, $F_{0.85}$	stress at secant modulus, 0.7 E or 0.85 E of skin material
D	flexural stiffness of skin per inch of width, $Et_s^3/12(1-\nu^2)$
g	spacing between staggered columns of fasteners, in.

Definition of Symbols (Continued)

Symbol	Definition
G	elastic shear modulus, psi
h'	long-side dimension of rectangular tube, in.
h	spacing between staggered rows of fasteners, in.
I	bending moment of inertia of stiffener cross section taken about the stiffener centroidal axis, $in.^4$
I_p	polar moment of inertia of section about center of rotation, $in.^4$
J	torsion constant of the stiffener, $in.^4$ (GJ = torque/twist per unit length)
k	rotational spring constant
k_c	compressed skin local buckling coefficient
k_h, k_t, k_w	compressed stiffener local buckling coefficients.
k_s	shear buckling coefficient
k_{wr}	compressed panel wrinkling coefficient
k_{sc}	compressive-local-buckling coefficient for panels with integral stiffeners.
M. S.	margin of safety
N	number of stiffeners
n	shape parameter
r	radius, in.
s	fastener pitch, in.

Definition of Symbols (Continued)

Symbol	Definition
t	thickness, in.
η	plasticity reduction factor
$\bar{\eta}$	cladding reduction factor
ν	Poisson's ratio in elastic range
Γ	torsional-bending constant, in.^{6}
Subscript	
c	compression
e	effective
f	flange
t	tension or top web of hat-section stiffeners
s	skin, shear
w	web
av	average
cir	local compressive inter-fastener buckling
co	cutoff
CRI	local compressive integral stiffener panel buckling
cs	compressive skin buckling
csr	shear skin buckling

Definition of Symbols (Concluded)

Subscripts	Definition
csk	compressive local skin buckling
cst	compressive local stiffener buckling
ct	compressive panel torsional buckling
cw	compressive panel wrinkling
cy	compressive yield
tr	tensile fastener stress
pl	proportional limit

C4.2.0 Conventionally Stiffened Flat Panels in Compression

Buckling resulting from local compression instability in a panel conventionally stiffened (Fig. C4.2.0-1) in the direction of the load may occur in either the stiffener elements or the plate.

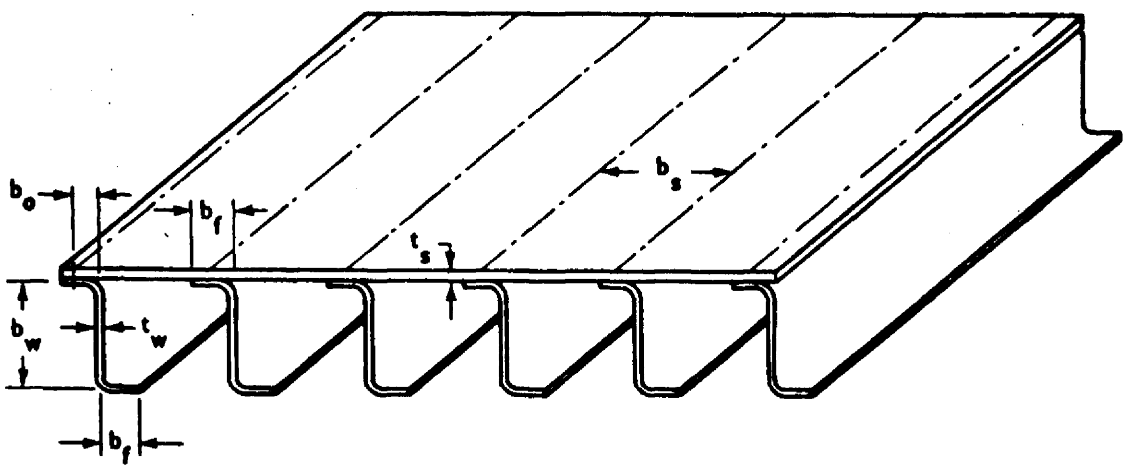

FIGURE C4.2.0-1. TYPICAL CONVENTIONALLY STIFFENED PANEL.

The forms of local instabilities and failures which will be discussed in this section are:

1. Local skin buckling
2. Local stiffener buckling
3. Inter-fastener buckling
4. Panel wrinkling (Forced crippling)
5. Torsional instability

Although these are distinct instability modes, ultimate buckling failure is usually a combination of two or more modes.

Other local modes of failure classified as column post-buckling phenomena are described in the following three paragraphs but are not discussed further in this section of the manual.

1. Stiffener crippling is a local collapse of a composite stiffener section. Crippling is covered in Section C1.3.1 of this manual.

2. Lateral instability consists of a twisting of the stiffener section, accompanied by a distortion of the cross section. The analytical technique presented in "Shell Analysis Manual" [1] is recommended to the reader since this mode is not discussed in this manual at the present time.

3. Monolithic panel failure, an extension of stiffener crippling, is a failure of skin and stiffener so fastened together that they act as a monolithic unit when subjected to crippling stress levels. Analytical methods presented in the documents cited in References 2 and 3 are recommended to the reader since this mode is not discussed in this manual at the present time.

Three of the cited local instability modes are a direct function of the fastener spacing (Fig. C4.2.0-2).

C4.2.1 Local Skin Buckling

A local compression instability mode that is often observed is local skin buckling. This mode can occur in skins between or under stiffeners of a stiffened panel. Although this mode can be a failure in itself, it usually precipitates failure in another mode if the load is appreciably increased.

The normal analytical procedure for this type instability is to treat the skin as a simply supported flat plate of infinite length. The following general equation for skin buckling stress is written in nondimensional form:

$$\frac{F_{csk}}{F_{0.7}} = \eta \bar{\eta} \frac{k_c \pi^2 E}{12(1-\nu^2) F_{0.7}} \left(\frac{t_s}{b}\right)^2 \quad . \qquad (1)$$

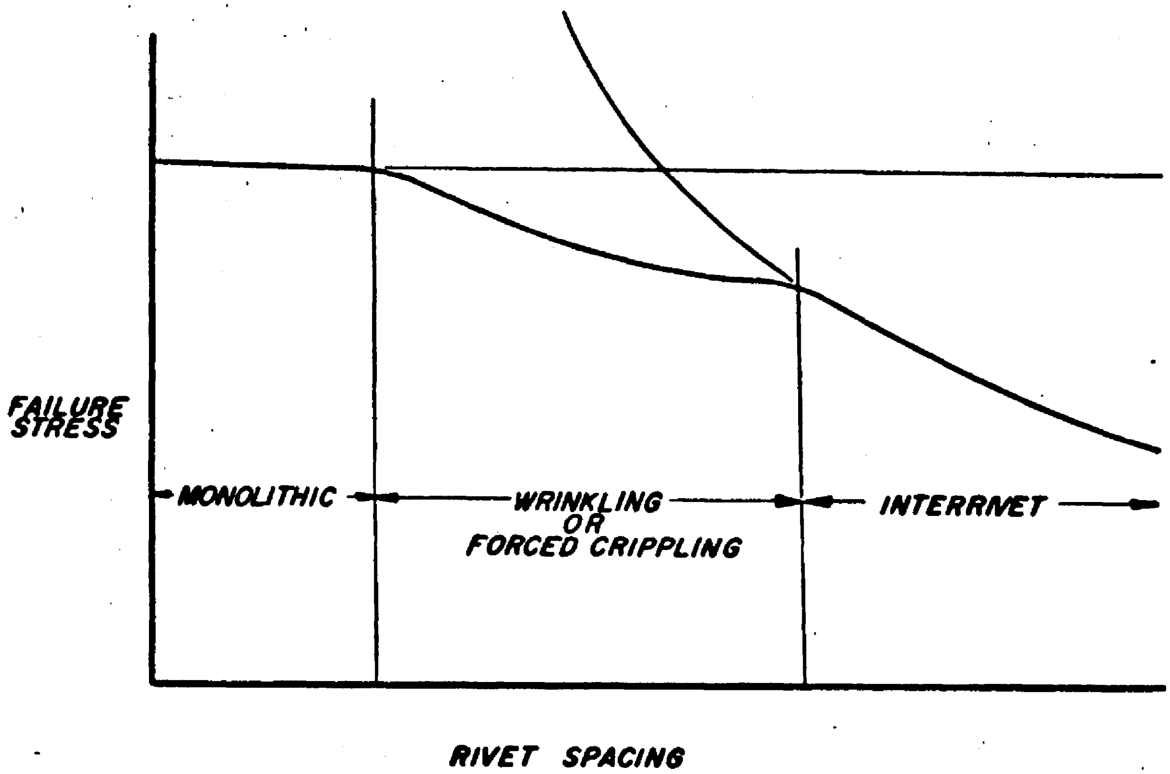

FIGURE C4. 2. 0-2. FAILURE MODES OF SHORT RIVETED PANELS.

This equation can be solved by the following procedure:

1. Determine $F_{0.7}$ from appropriate stress-strain curve.

2. Determine k_c from Table C2. 1. 5. 5.

3. Determine n from Table C2. 1. 5. 6. If n is not given in the table, it may be obtained from data given in Section C4. 2. 3.

4. Calculate $\dfrac{k_c \pi^2 E}{12\,(1-\nu^2)\,F_{0.7}} \left(\dfrac{t_s}{b}\right)^2$.

5. Enter Figure C2. 1. 5-4 at value calculated in step four to obtain $F_{csk}/F_{0.7}$, using appropriate n curve.

6. Calculate F_{csk} .

F_{csk} should include plasticity and cladding reduction factors, as given in Tables C2.1.5.1 and C2.1.5.2 respectively, if applicable.

The margin of safety, M.S., can be calculated as follows:

$$M.S. = \frac{F_{csk}}{f_c} - 1 \quad , \tag{2}$$

where f_c is the compressive stress in the skin.

C4.2.2 Local Stiffener Buckling

Local instability or local buckling of a section is to be distinguished from crippling of a section. Crippling is an ultimate type of failure (discussed in Section C1.3.1), while local buckling is an elastic condition which may occur at much lower stresses. Generally, this type of instability will not constitute failure in itself but will usually precipitate failure in another mode.

In stiffeners with flat sides, local instability is defined as that mode of distortion in which the meets of adjoining sides remain stationary. Thus, each side buckles as a plate whose edges parallel to the load rotate through the same angles as those of the adjoining sides and the half-wavelength is of the order of the cross-section dimensions (Fig. C4.2.2-1).

Two of the simplest flange-web shapes are angles and zees. These can be considered as compound plate elements and can be broken up as shown in Figure C4.2.2-2. Information found in Section C2 can be used to determine buckling stresses of the shapes described above.

However, a more direct method for predicting the local buckling stress, taking into account the interaction of the sides, in the elastic range is to use the following equation:

$$F_{cst} = \eta \bar{\eta} \frac{k_i \pi^2 E}{12 (1-\nu^2)} \left(\frac{t}{b}\right)^2 , \qquad (3)$$

where (k_i) is an experimentally determined local buckling coefficient. Figures C4.2.2.-3 through C4.2.2-6 show (k_i) values for various channels, Z-sections, H-sections, rectangular-tube-sections, and hat-sections often used for stiffened-plate construction.

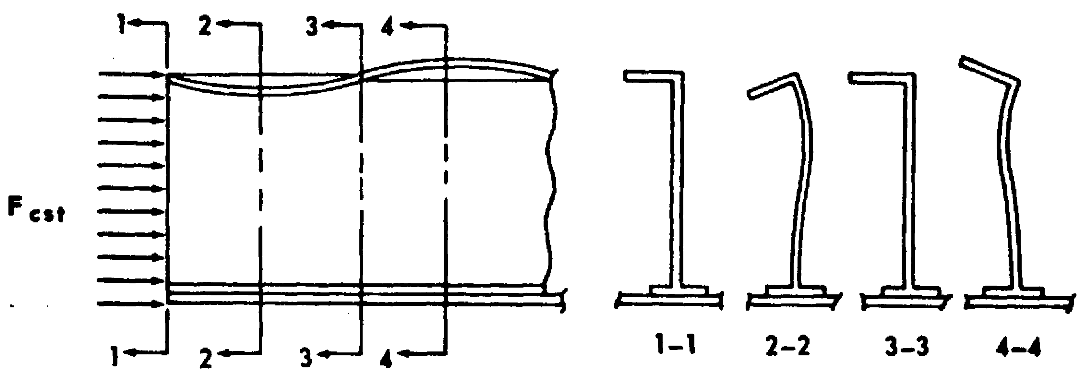

FIGURE C4.2.2-1. TYPICAL STIFFENER LOCAL BUCKLING SHOWING ONLY TWO HALF-WAVES.

A discussion of cladding and plasticity-reduction factors can be found in Section C2.1.1. Figure C4.2.2-7 gives experimentally determined plasticity-reduction factors for stiffener shapes presented in Figures C4.2.2-3 through C4.2.2-6.

The reader should also observe dimensioning differences for formed and extruded stiffeners, as shown in Figure C4.2.2-8, prior to calculating parameters when using the buckling coefficient curves cited above.

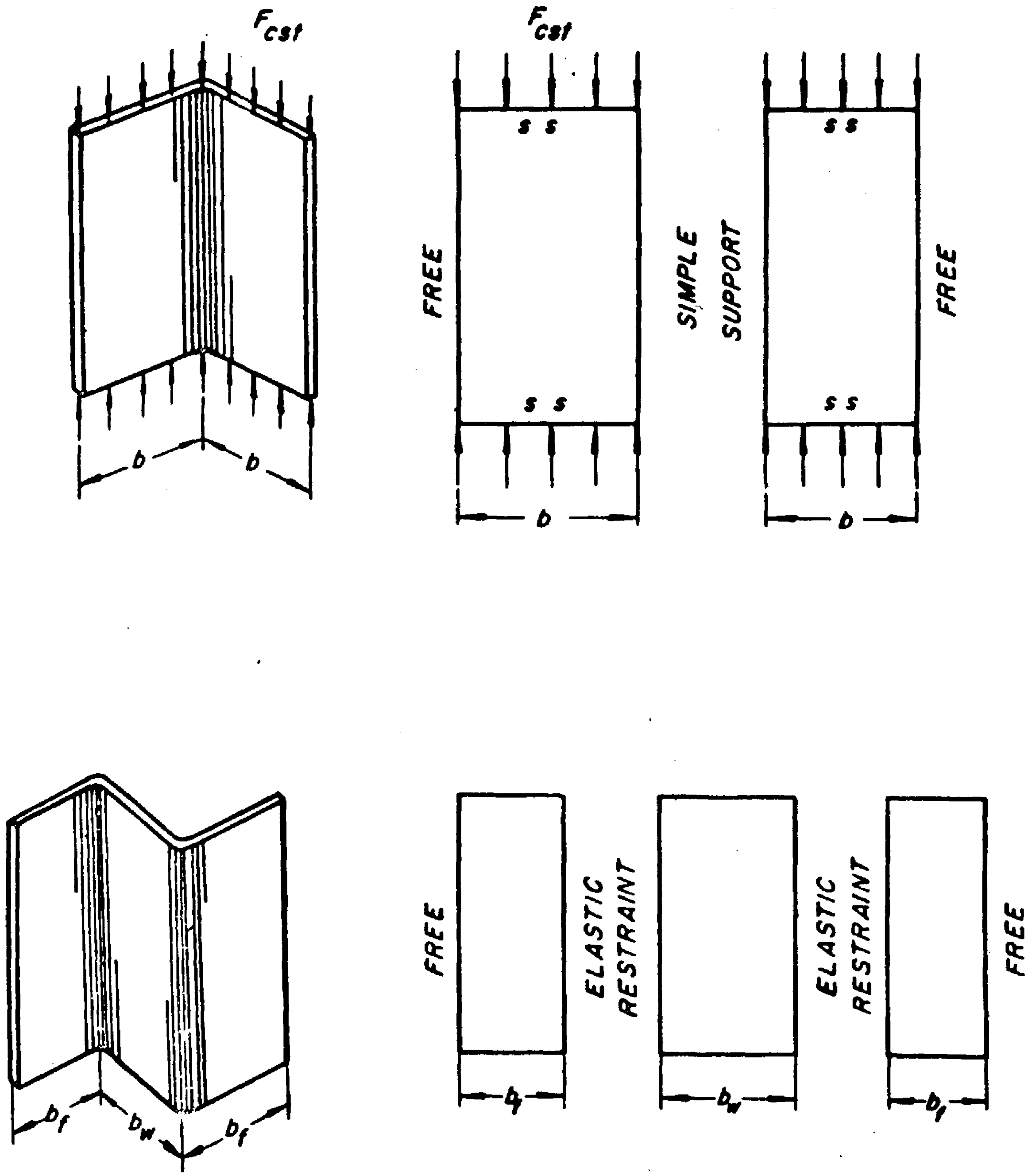

FIGURE C4.2.2-2. BREAKDOWN OF ANGLE AND Z-STIFFENERS INTO COMPONENT PLATE ELEMENTS.

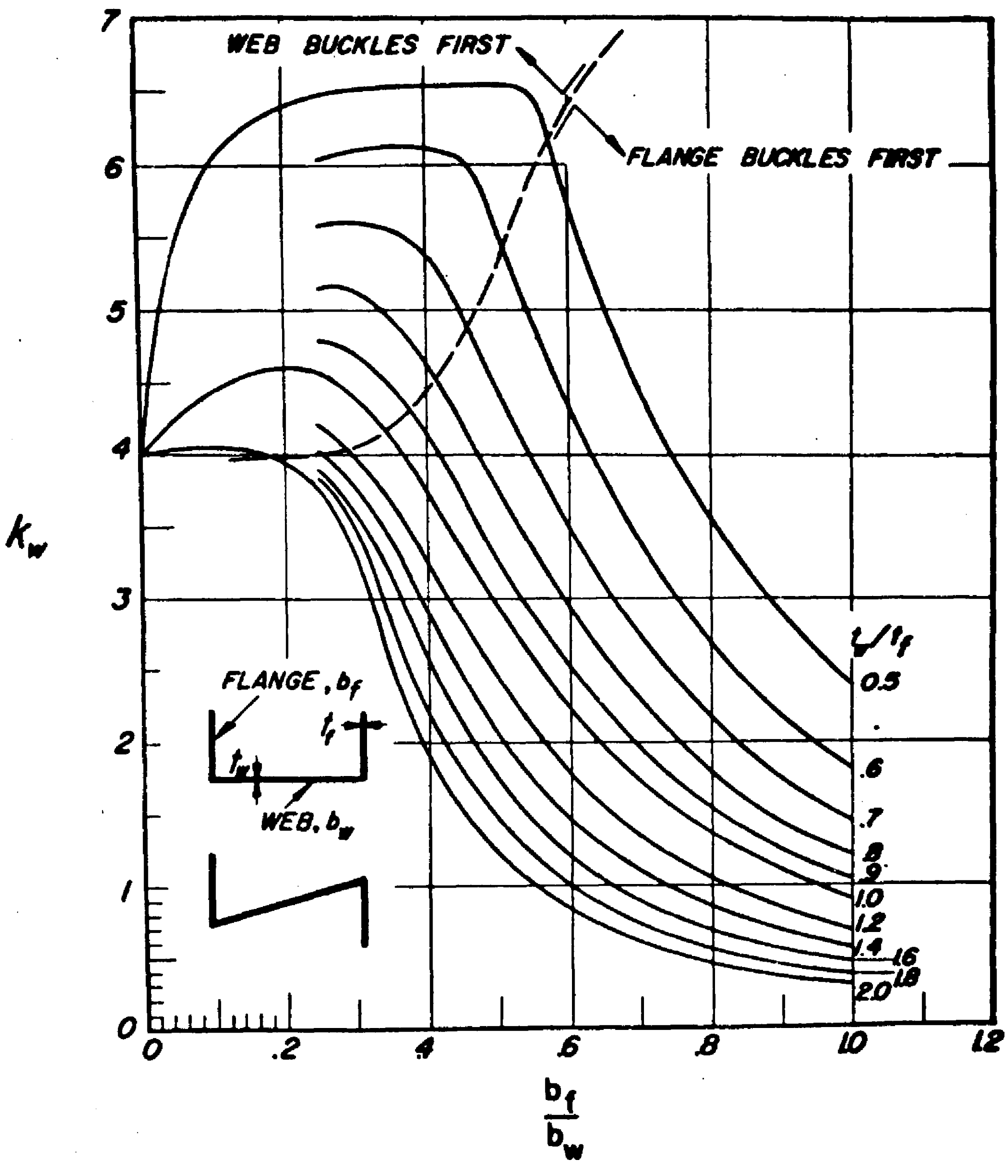

$$F_{cst} = \eta \bar{\eta} \frac{k_w \pi^2 E}{12 (1 - \nu^2)} \left(\frac{t_w}{b_w} \right)^2$$

FIGURE C4. 2. 2-3. COMPRESSION LOCAL BUCKLING COEFFICIENTS FOR CHANNEL AND Z-SECTION STIFFENERS.

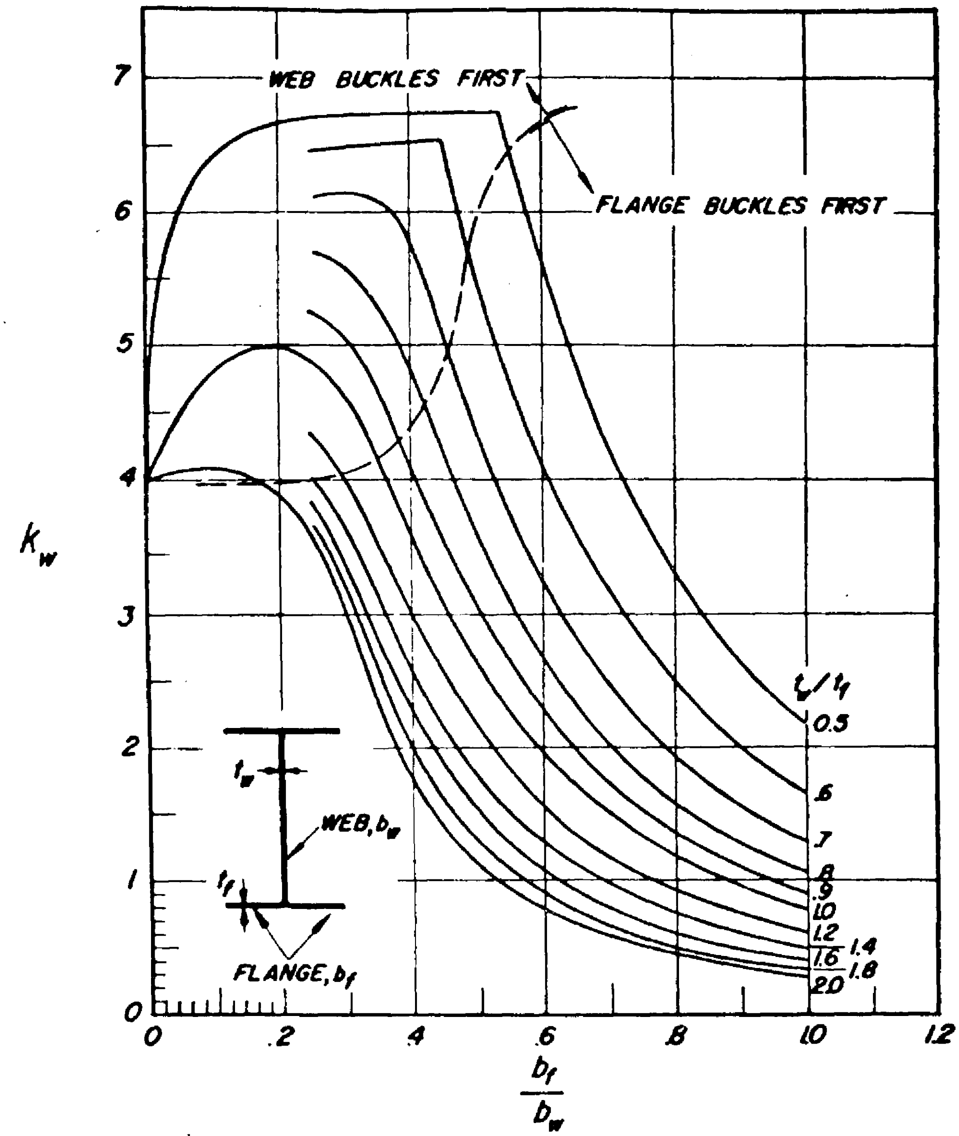

$$F_{cst} = \eta \bar{\eta} \frac{k_w \pi^2 E}{12 (1 - \nu^2)} \left(\frac{t_w}{b_w} \right)^2$$

FIGURE C4.2.2-4. COMPRESSION LOCAL BUCKLING COEFFICIENT FOR H-SECTION STIFFENERS.

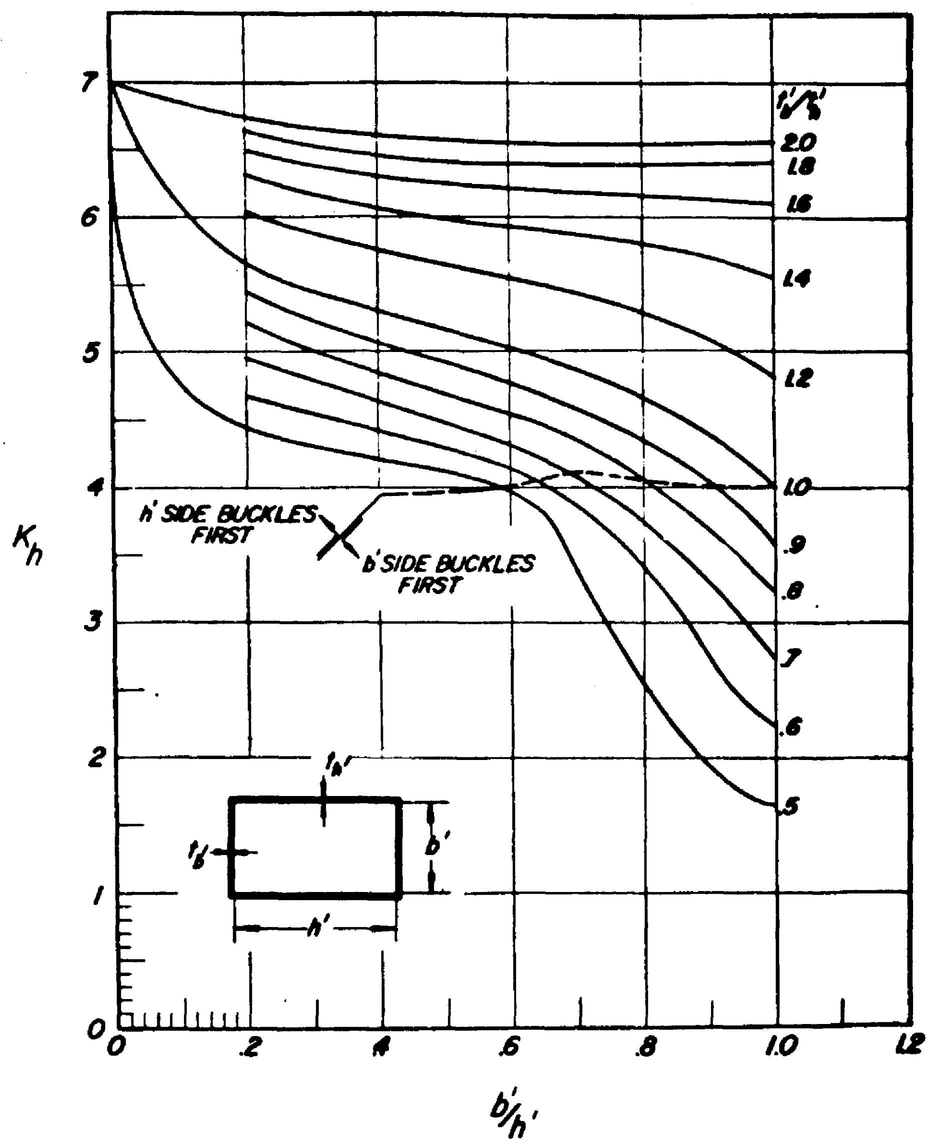

$$F_{cst} = \eta \bar{\eta} \frac{k_h \pi^2 E}{12(1-\nu^2)} \left(\frac{t_{h'}}{h'}\right)^2$$

FIGURE C4.2.2-5. COMPRESSION LOCAL BUCKLING COEFFICIENT FOR RECTANGULAR-TUBE-SECTION STIFFENERS.

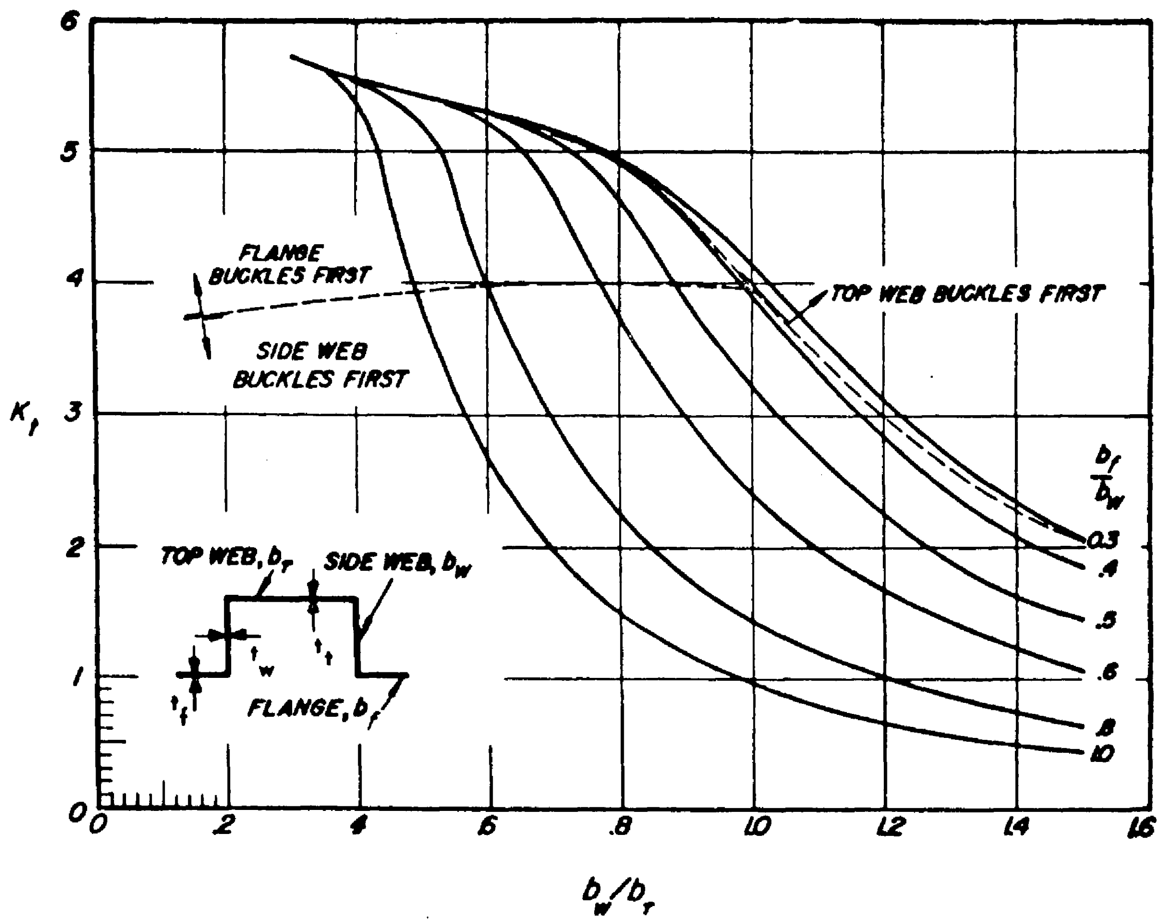

$$F_{cst} = \eta \bar{\eta} \frac{k_t \pi^2 E}{12 (1 - \nu^2)} \left(\frac{t}{b_T}\right)^2$$

FIGURE C4.2.2-6. COMPRESSION LOCAL BUCKLING COEFFICIENT FOR HAT-SECTION STIFFENERS, $t = t_f = t_w = t_t$.

Fig.	Section	Buckling coefficient	Plasticity-reduction factor
C4.2.2-3	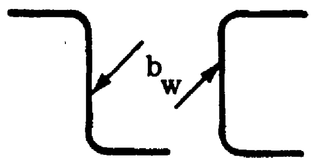	k_w	$(E_s/E)(1-\nu_e^2)/(1-\nu^2)$ is about 5 percent conservative
C4.2.2-4	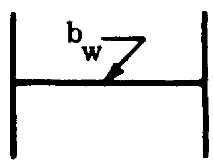	k_w	None reported
C4.2.2-5	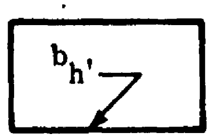	k_h	None reported
C4.2.2-6	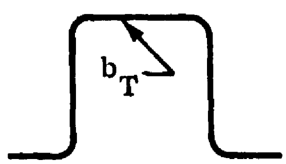	k_t	None reported

FIGURE C4.2.2-7. EXPERIMENTALLY DETERMINED PLASTICITY-REDUCTION FACTORS FOR COMPOSITE SHAPES IN FIGURES C4.2.2-3 THROUGH C4.2.2-6.

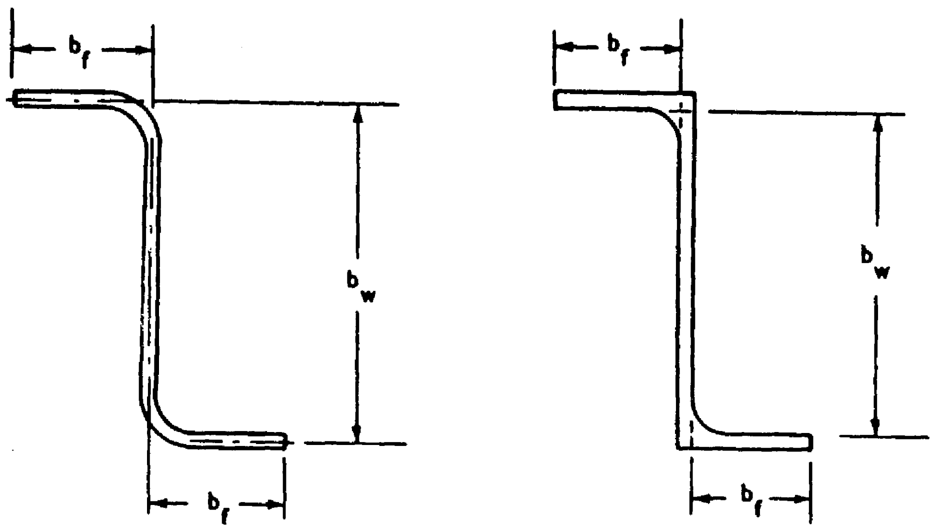

(a) Formed Section (b) Extruded Section

FIGURE C4.2.2-8. TYPICAL DIMENSION FOR FORMED AND EXTRUDED STIFFENERS.

C4.2.3 Inter-Fastener Buckling (Interrivet Buckling)

This mode of local instability, as shown in Figure C4.2.3-1, occurs between fasteners in the skin of longitudinally stiffened panels in compression, causing a separation between the skin and an essentially undistorted stiffener. The action approximates that of a wide column with a width equal to or less than the fastener spacing. Inter-fastener buckling is usually found in stiffened-panel designs where the skin gage is less than the stiffener gage. Any increase in load above the inter-fastener buckling load cannot be supported by the skin; therefore, redistribution of load to the stiffeners and excessive skin deformation occurs.

A criterion for fastener spacing is determined from test data which result from failure in the inter-fastener buckling mode rather from panel

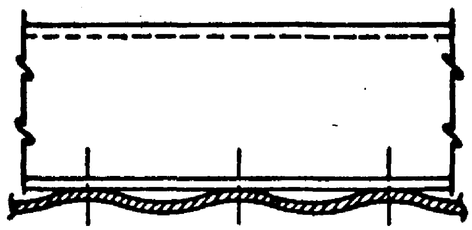

FIGURE C4.2.3-1. TYPICAL INTER-FASTENER BUCKLING.

wrinkling (Section C4.2.4):

$$s/b_s \geq 1.27/(k_{wr})^{1/2} \quad , \qquad (4)$$

where the wrinkling coefficient (k_{wr}) is given in Section C4.2.4. This coefficient is a function of the experimentally determined effective rivet offset (f) . Dimensioning rules given in Figure C4.2.2-8 for formed and extruded stiffener sections should be observed.

When inter-fastener buckling is analyzed as a wide column, the following equation applies:

$$F_{cir} = \eta \bar{\eta} \frac{e \pi^2 E_c}{12 (1-\nu^2)} \left(\frac{t_s}{s}\right)^2 \quad . \qquad (5)$$

Figure C4.2.3-2 presents a graphical nondimensional form of the equation above. The values needed to enter this chart are: $F_{0.70}$, $F_{0.85}$, E_c , ν , t_s , s , e, and n.

Values of $F_{0.70}$ and $F_{0.85}$ may be obtained from a stress-strain curve as indicated in Figure C4.2.3-3 (a). Values for E_c and ν can be obtained from MIL-HDBK-5A or other well-qualified sources.

If cladding is used on the sheet, the sheet thickness, t_s , will not include the cladding material. The fastener spacing to be used will depend on the pattern of the fasteners. For a single row or double rows the fastener spacing will be the actual distance between fasteners, as shown in Figures C4.2.3-4 (a) and C4.2.3-4 (b). For staggered rows, an effective fastener spacing must be used. This effective spacing, s, may be calculated:

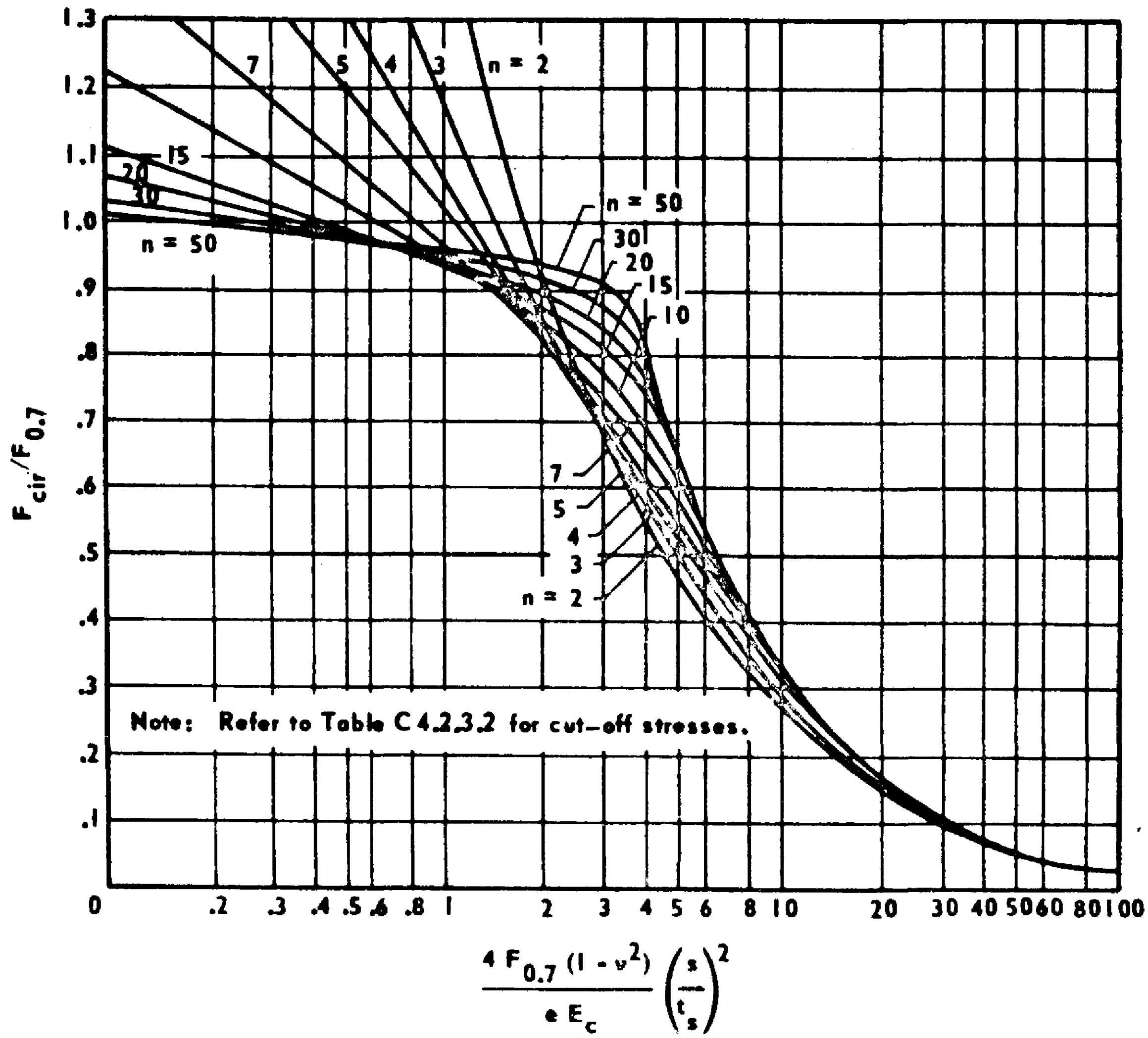

FIGURE C4. 2. 3-2. CHART OF NONDIMENSIONAL INTERRIVET BUCKLING STRESS.

$$s = \frac{g}{2} + h \qquad (0 \le g \le 2s) \qquad , \qquad (6)$$

where g and h are shown in Figure C4. 2. 3-4 (c). If g is greater than 2h, use 2h as the value of s.

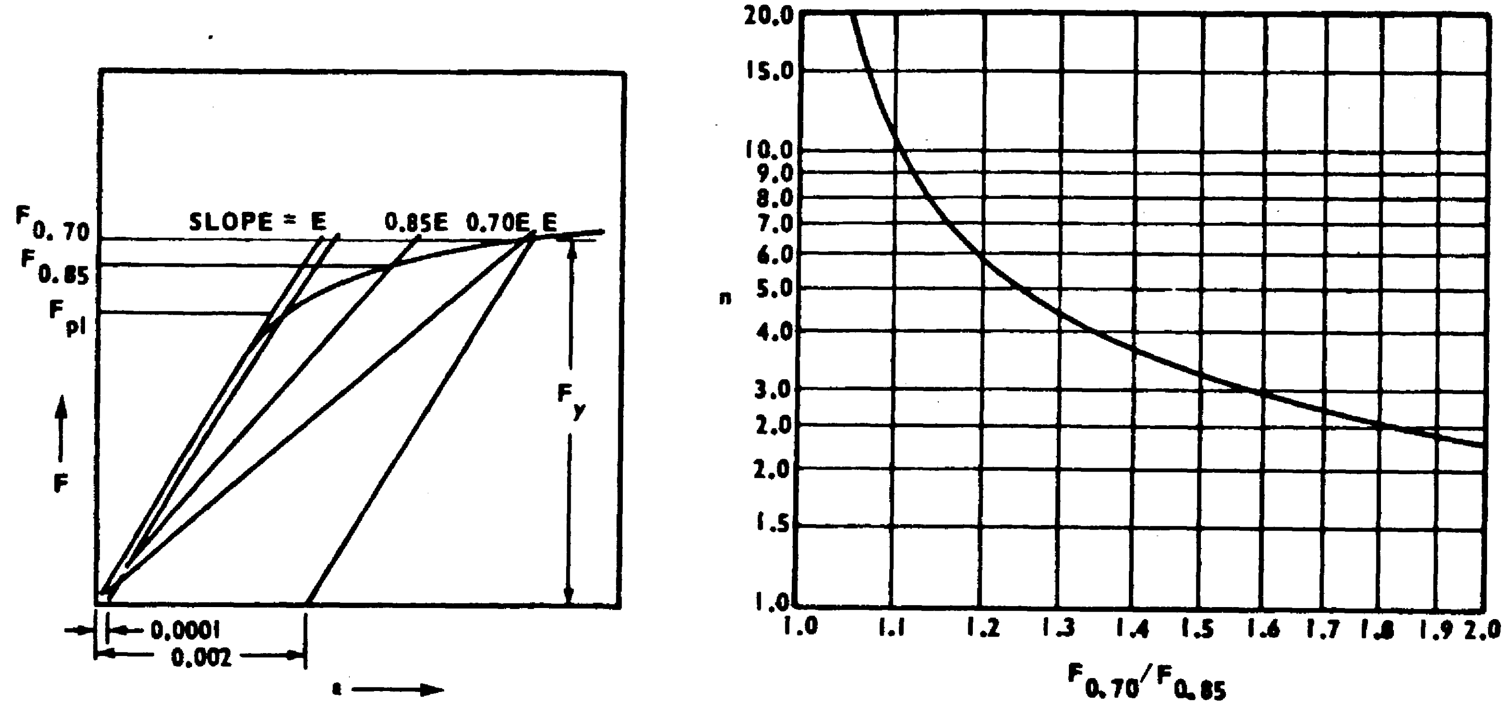

(a) Significant Stress Quantities on a Typical Stress-Strain Curve.

(b) Dependence of Shape Factor on Ratio $F_{0.70}/F_{0.85}$.

$$n = 1 + \log_e (17/7)/\log_e (F_{0.70}/F_{0.85}) .$$

FIGURE C4.2.3-3. CHARACTERISTICS OF STRESS-STRAIN CURVES FOR STRUCTURAL ALLOYS DEPICTING QUANTITIES USED IN THREE-PARAMETER METHOD.

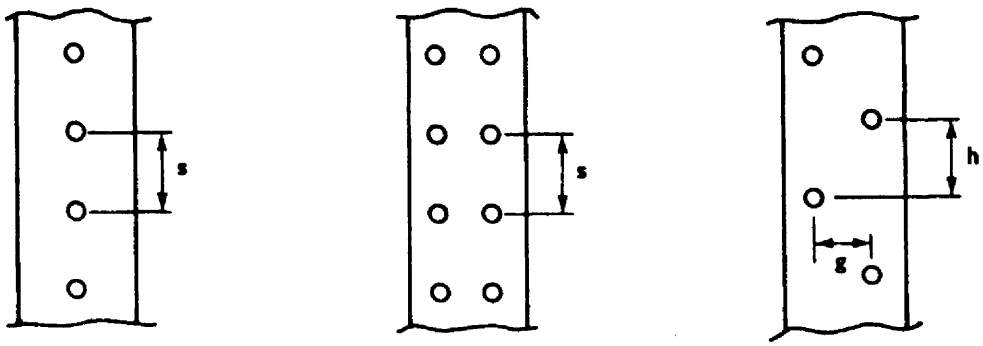

(a) Single row (b) Double rows (c) Staggered rows

FIGURE C4.2.3-4. FASTENER SPACINGS FOR TYPICAL FASTENER PATTERNS.

The value of e is dependent on the type of fastener. Values of e to be used are listed in Table C4.2.3.1 for several types of fasteners.

Values of the shape parameter n for several materials are given in Table C2.1.5.6. For materials not given, the shape parameter may be obtained from Figure C4.2.3-3 (b). If n is out of the range of the curve in that figure, it may be calculated from the following equation:

Table C4.2.3.1. Values of End-Fixity Coefficient "e" for Several Types of Fasteners

Type of Fastener	e
Flathead rivet	4
Spotweld	3.5
Brazierhead rivet	3
Machine csk. rivet	1
Dimpled rivet	1

$$n = 1 + \log_e (17/7)/\log_e (F_{0.70}/F_{0.85}) \quad . \tag{7}$$

For temperatures other than room temperature, the analysis may be performed using the values of F_{cy}, $F_{0.70}$, $F_{0.85}$ and n for this temperature. These values can be obtained from the appropriate stress-strain curve.

It should be noted that a cutoff stress is used in the interrivet buckling calculations. The values of the cutoff stress recommended for use here are shown in Table C4.2.3.2.

Table C4.2.3.2. Recommended Values for Cutoff Stress

Material	Cutoff Stress (F_{co})
2024-T, 2014-T, 6061-T	$F_{cy}\left[1 + \frac{F_{cy}}{200,000}\right]$
7075-T	$1.075\ F_{cy}$
18-8 (1/2 H)*	$0.835\ F_{cy}$
(3/4 H)	$0.875\ F_{cy}$
(FH)	$0.866\ F_{cy}$
All other materials	F_{cy}

* Cold-rolled, with grain, based on MIL-HDBK-5A properties.

A general procedure for calculating inter-fastener buckling stress and margin of safety is listed below:

1. Determine $F_{0.70}$ and $F_{0.85}$ from appropriate stress-strain curve.
2. Determine n from Table C2.1.5.6. If n is not given in the table,

it may be obtained from Figure C4.2.3-3 (b) or equation (7).

3. Obtain e from Table C4.2.3.1 .

4. Calculate $\frac{4 F_{0.7} (1 - \nu^2)}{e E_c} \left(\frac{s}{t_s} \right)^2$.

5. Enter Figure C4.2.3-2 at value calculated in step four to obtain $F_{cir}/F_{0.7}$ using the appropriate n curve.

6. Calculate F_{cir} as

$$F_{cir} = (F_{0.7}) \text{ (Value determined in step five)} .$$

7. Obtain the cutoff stress, F_{co}, from Table C4.2.3.2.

8. Calculate the M.S. as

$$M.S. = \frac{F_{cr}}{f_c} - 1 ,$$

where F_{cr} is the lower of the two values F_{cir} and F_{co}, and f_c is the compressive sheet stress between fasteners.

C.4.2.4 Panel Wrinkling (Forced Crippling)

A mode of local instability failure sometimes encountered when designing stiffened panels is panel wrinkling. This generally occurs in designs where the skin gage is equal to or greater than the stiffener gage.

This mode of failure, shown in Figure C4.2.4-1, results from the existence of a flexible attachment between the skin and stiffener. The skin acts as a column supported at the fastener attachment points on an elastic foundation. The elastic foundation is provided by the stiffener attachment flange to a degree dependent on its geometry: the offset distance of the

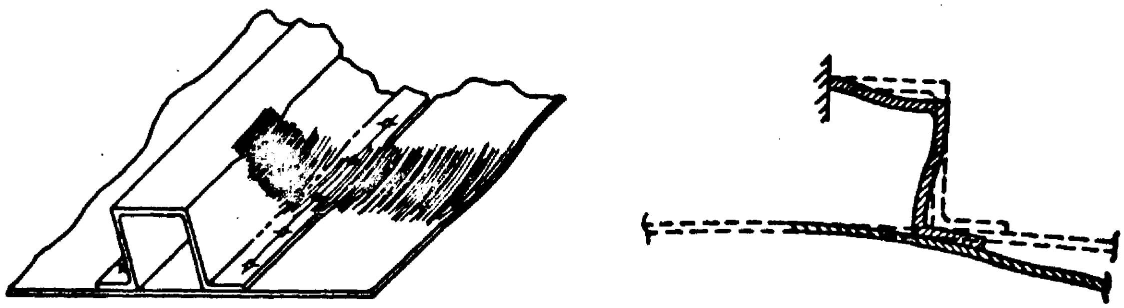

(a) General Appearance of a Wrinkling Failure

(b) A Cross Section at Wrinkle Showing Distortions of Stiffener and Skin

FIGURE C4.2.4-1. TYPICAL PANEL WRINKLING FAILURE.

fastener from the stiffener web, the fastener spacing, diameter, and strength. In the wrinkling mode, the attachment flange of the stiffener follows the skin contour and causes other plate elements of the stiffener to distort, thereby precipitating failure of the panel as a whole.

The most commonly used analytical method for determining wrinkling-buckling stresses is semiempirical in nature. The general equation for wrinkling is

$$F_{cw} = \eta \bar{\eta} \frac{k_{wr} \pi^2 E_c}{12 (1 - \nu^2)} \left(\frac{t_s}{b_s}\right)^2 , \qquad (8)$$

where k_{wr}, the wrinkling coefficient is given in Figure C4.2.4-2. This coefficient is a function of the experimentally determined effective rivet offset (f) which is obtained from Figure C4.2.4-3. Dimensioning rules given in Figure C4.2.2-8 for formed and extruded stiffener sections should be observed. Cladding ($\bar{\eta}$) and plasticity (η) correction factors should be determined in agreement with Section C2.1.1 and should be used accordingly.

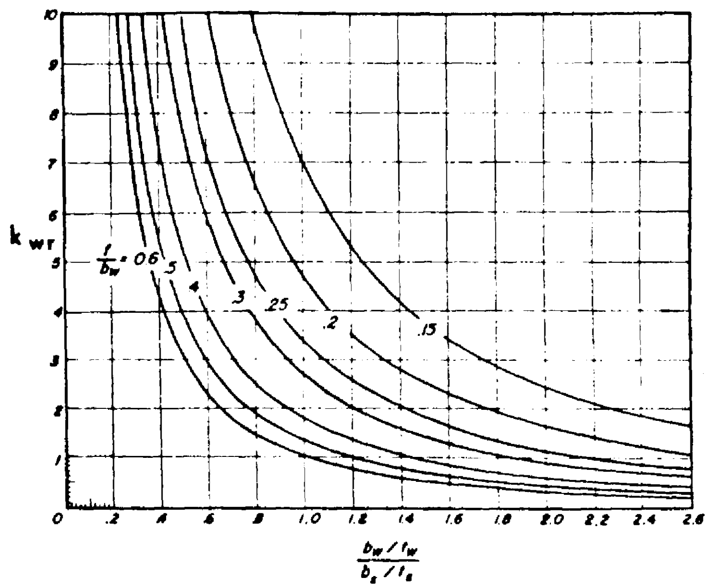

FIGURE C4.2.4-2. EXPERIMENTALLY DETERMINED BUCKLING COEFFICIENT FOR FAILURE IN THE WRINKLING MODE.

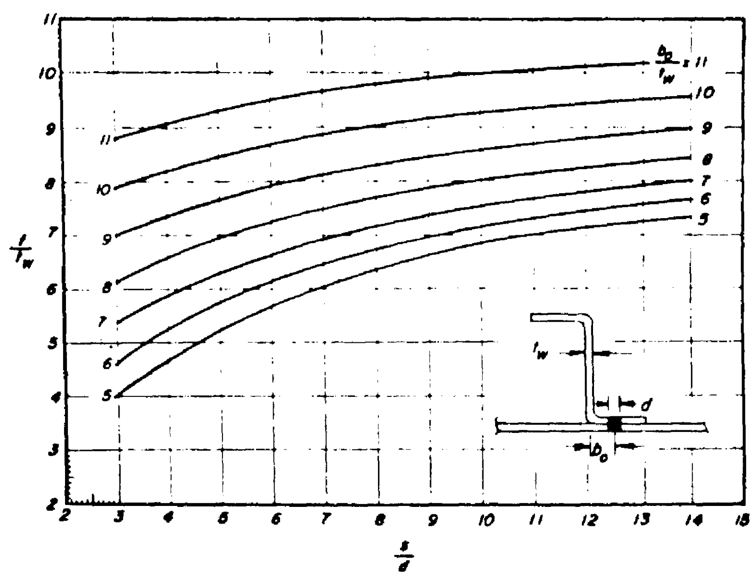

FIGURE C4.2.4-3. EXPERIMENTALLY DETERMINED VALUES OF EFFECTIVE RIVET OFFSET.

A criterion for fastener spacing is determined from test data which result from a wrinkling mode failure:

$$s/b_s < 1.27/(k_{wr})^{1/2} \quad . \qquad (9)$$

Wrinkling imposes a high tensile load on the fasteners which are required to make the stiffener attachment flange conform to the wrinkled sheet. An approximate expression for the tensile strength of the fastener is

$$f_{tr} > \frac{0.7}{E_{st}} \frac{b_s}{d} \frac{s}{d} \left(F_{cw}\right)^2 \quad . \qquad (10)$$

The tensile strength of the fastener (F_{tr}) is defined in terms of the shank area, and it may be associated with either shank failure or pulling of the countersunk head of the fastener through the sheet.

When the fasteners that are being analyzed are rivets of materials other than 2117-T4 aluminum alloy, the following experimentally proven expressions should be used.

For 2117-T4 rivets whose tensile strength is $F_t = 57$ ksi , the criteria are:

$$F_t = 57 \text{ ksi} \quad , \qquad (11)$$

if $\quad d_e/t_{av} \leqq 1.67 \quad ;$

or

$$F_t = \frac{190}{d_e/t_{av}} - \frac{160}{(d_e/t_{av})^2} \quad , \qquad (12)$$

if $d_e/t_{av} > 1.67$;

where t_{av} (in inches) is the average of sheet and stiffener thickness. The effective diameter d_e is the diameter for a rivet made from 2117-T4 material.

The effective diameter of a rivet of another material is,

$$d_e/d = (F_{tr}/F_t)^{\frac{1}{2}} \quad , \tag{13}$$

where F_{tr} is the tensile strength of a rivet, defined as maximum tensile load divided by shank area in ksi units.

The following procedure is recommended when analyzing a panel for wrinkling:

1. Calculate s/d.

2. Enter Figure C4.2.4-3 at value calculated in step 1 to obtain f/t_w, using the appropriate b_e/t_w curve.

3. Calculate 1.

4. Calculate $\dfrac{b_w/t_w}{b_s/t_s}$.

5. Enter Figure C4.2.4-2 at value calculated in step 4 to obtain k_{wr} using the appropriate f/b_w curve.

6. Solve equation (9).

   a. If equation is satisfied, continue to step 7.

   b. If equation is not satisfied, wrinkling is not the critical mode; return to Section C4.2.3.

7. Calculate F_{cw} using equation (8).

8. Check fastener tensile stresses using equation (10), and equations (11), (12), and (13) if necessary.

9. Calculate the panel M.S. as

$$M.S. = \frac{F_{cw}}{f_c} - 1 ,$$

where f_c is the compressive stress in the skin, and the fastener M.S. is

$$M.S. = \frac{F_{tr}}{f_{tr}} - 1 ,$$

where F_{tr} is the tensile allowable of the fastener.

C4.2.5 Torsional Instability

Torsional instability of a stiffened panel between frames occurs when the cross section of the stiffener rotates but does not distort or translate in its own plane. Typical antisymmetric and symmetric torsional modes of instability are shown in Figure C4.2.5-1.

The analysis methods of torsional instability of stiffeners attached to sheets, as suggested in Reference 4, will be described. For the case of flat plates or cylinders with typical frame spacing,

$$d_f > \pi \left(E\eta_G I/k\right)^{\frac{1}{4}} , \qquad (14)$$

the allowable torsional instability stress, F_{ct}, for the mode shown in Figure C4.2.5-1 is

$$F_{ct} = G\eta_A \left[\frac{J}{I_p}\right] + 2\left[\frac{\sqrt{\Gamma}}{I_p}\right]\sqrt{E\eta_G k} , \qquad (15)$$

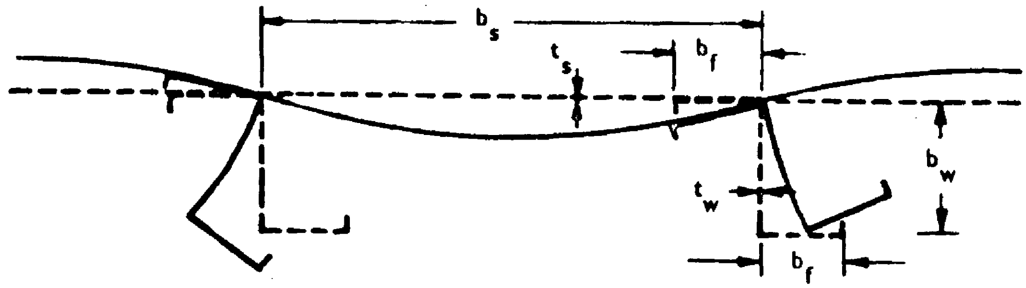

(a) Antisymmetric

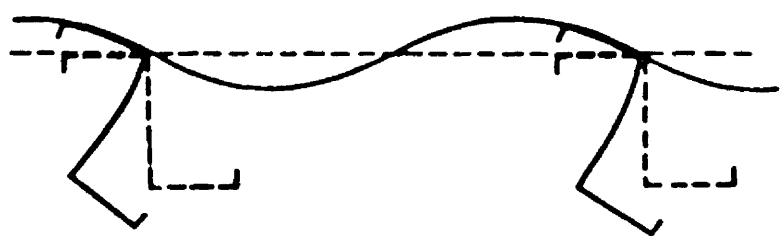

(b) Symmetric

FIGURE C4.2.5-1. MODES OF TORSIONAL INSTABILITY.

where $\frac{J}{I_p}$ and $\frac{\sqrt{\Gamma}}{I_p}$ values for Z and J type stiffeners may be obtained from Figures C4.2.5-2 and C4.2.5-3, respectively.

The plasticity correction factors η_A and η_G may be calculated by an iterative procedure using stress-strain curves (which can be found in MIL-HDBK-5A for most materials) for the given material and by the following expressions:

$$\eta_A = E_s/E \tag{16}$$

$$\eta_G = E_T/E \tag{17}$$

Curves for η_A and η_G for several materials at various temperature levels

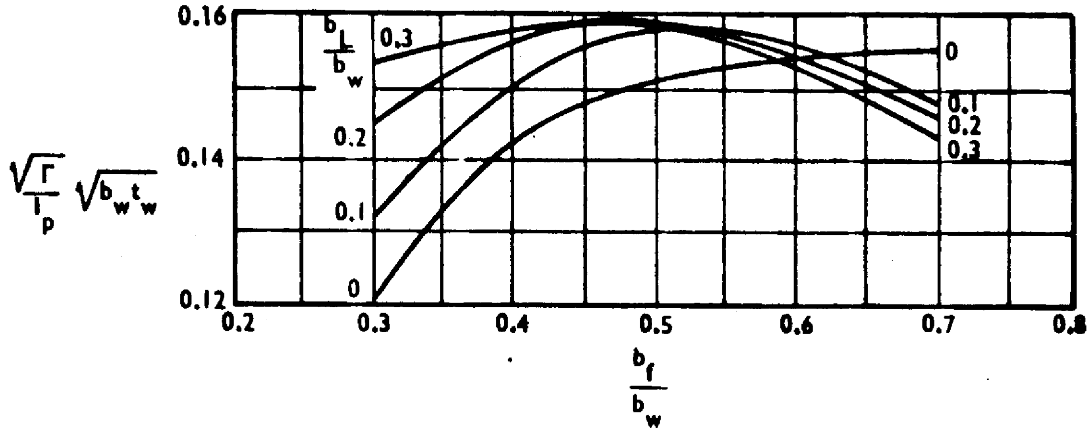

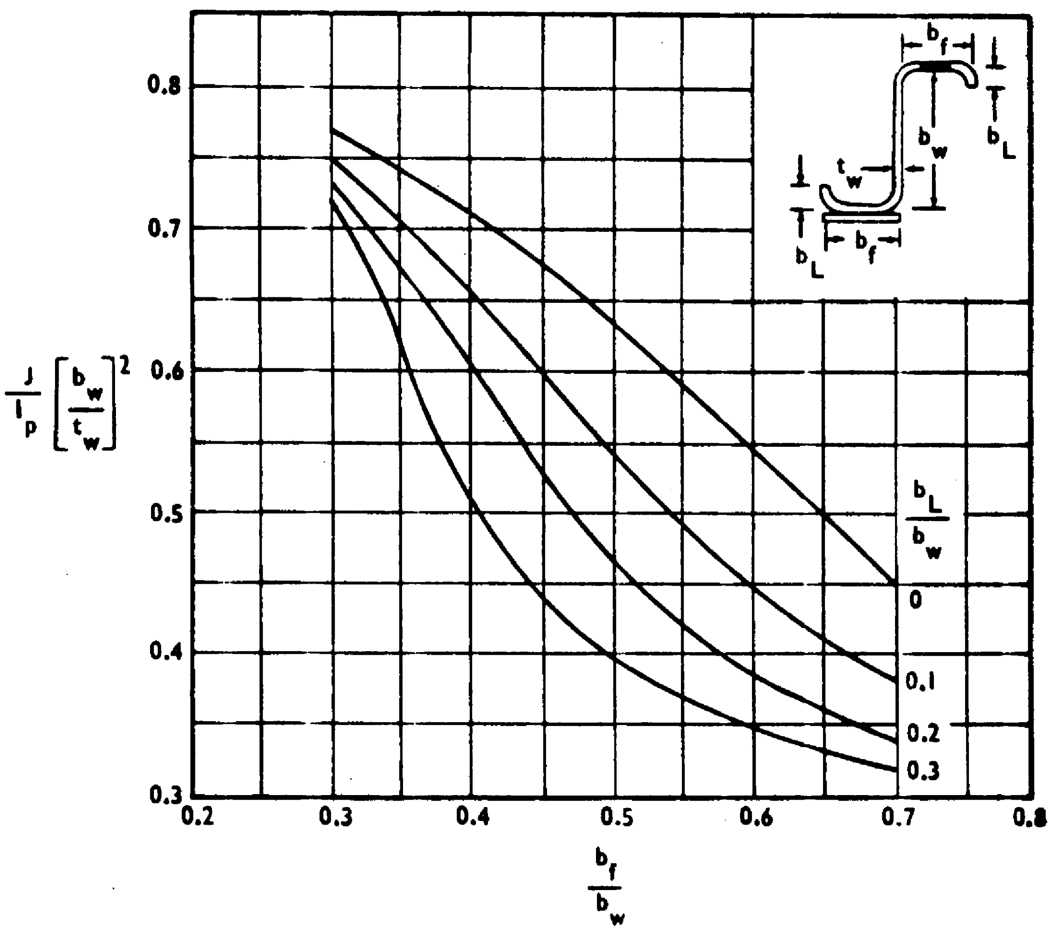

FIGURE C4. 2. 5-2. TORSIONAL SECTION PROPERTIES FOR LIPPED Z-STIFFENER-SHEET PANELS.

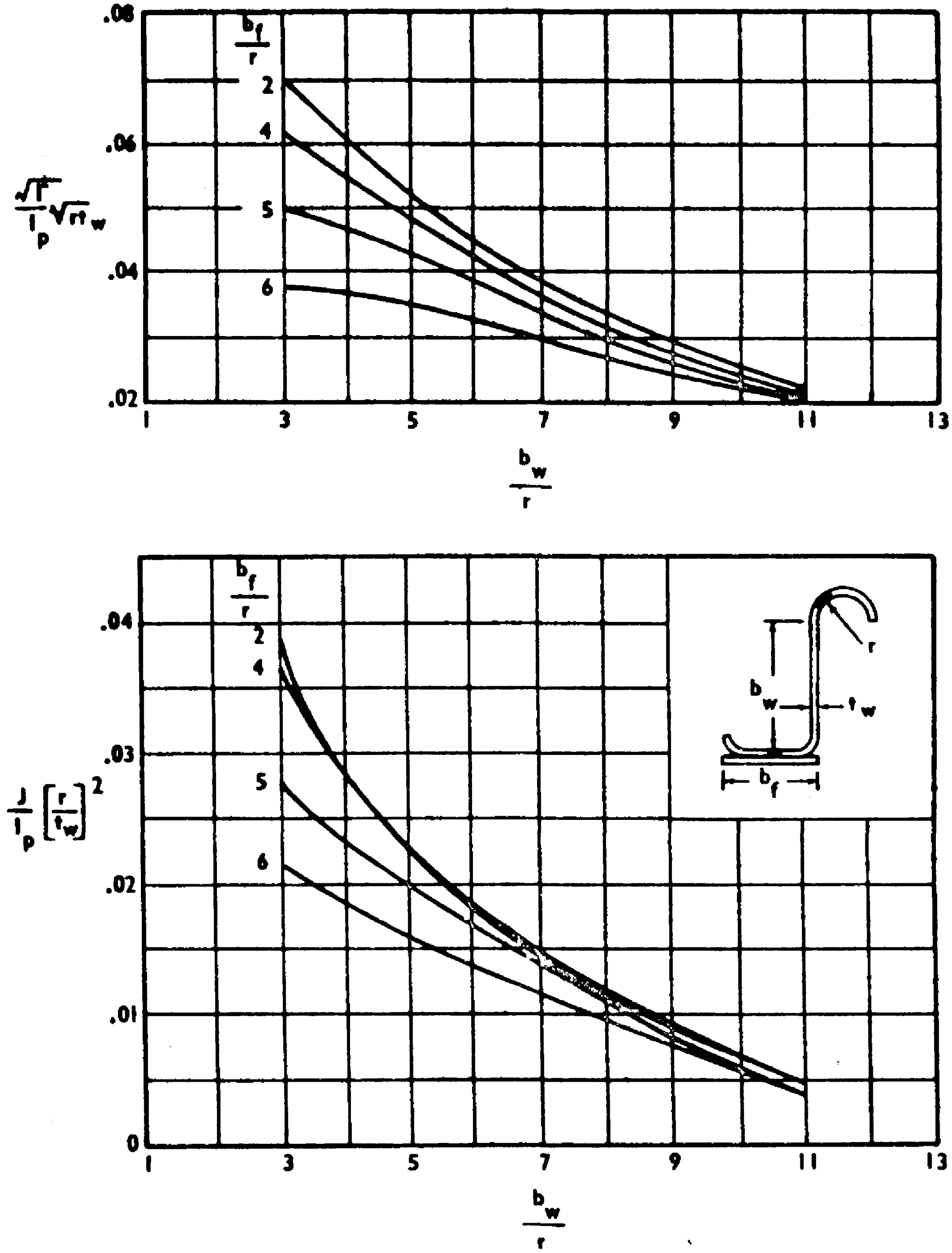

FIGURE C4.2.5-3. TORSIONAL SECTION PROPERTIES FOR J STIFFENER-SHEET PANELS.

may be found in References 1 and 5. Similar curves will be provided in Section C2.1.0 of this manual at a later date.

The rotational spring constant (k) may be found using the following expression:

$$\frac{1}{k} = \frac{1}{k_{web}} + \frac{1}{k_{sheet}} , \tag{18}$$

where

$$k_{web} = \frac{E t_w^3}{4 b_w + 6 b_f} \tag{19}$$

$$k_{sheet} = \frac{\lambda E t_s^3}{b_s} \tag{20}$$

$$\lambda = 1 \text{ for the symmetric mode} \tag{21}$$

$$\lambda = \frac{1}{3} \left[1 + 0.6 \frac{(F_{ct} - F_{crs})}{F_{crs}} \right] \tag{22}$$

for the antisymmetric mode.

If $F_{ct} < 4.33 F_{crs}$, the antisymmetric mode is critical. If $F_{ct} > 4.33 F_{crs}$, the symmetric mode of failure is critical. Since λ, η_A, and η_G depend on F_{ct}, the solution for F_{ct} is, in general, a trial-and-error procedure. Starting with the assumption that $\lambda = 1$, $\eta_A = \eta_G = 1$, calculate F_{ct} and correct for plasticity if required. Correct λ if required and repeat procedure until desired convergence is obtained. Then check to see whether or not $d_f > \pi \left(\frac{E\eta_G \Gamma}{k}\right)^{1/4}$.

If $d_f < \pi \left(\frac{E\eta_G \Gamma}{k}\right)^{1/4}$ the torsional instability stress is

$$F_{ct} = G\eta_A \left(\frac{J}{I_p}\right) + \frac{E\eta_G \Gamma}{I_p} \left(\frac{\pi}{d_f}\right)^2 + \frac{k(d_f/\pi)^2}{I_p} , \qquad (23)$$

where

$$\Gamma = \left(\frac{\sqrt{\Gamma}}{I_p}\right)^2 I_p^{\,2} . \qquad (24)$$

The formulas which have been presented may be used for stiffeners with sections other than those shown in Figures C4.2.5-2 and C4.2.5-3 if the values of I_p, J and Γ are known.

C4.3.0 Integrally Stiffened Flat Panels in Compression

The allowable buckling stress for local compression instability of certain integrally stiffened plates loaded parallel to the integral stiffeners may be found by determining the buckling coefficient k_s from Figures C4.3.0-1 through C4.3.0-5 and solving the equation:

$$F_{CRI} = \eta \bar{\eta} \frac{k_s \pi^2 E_c}{12 (1 - \nu^2)} \left(\frac{t_s}{b_s} \right)^2 \quad . \qquad (25)$$

The integral shapes presented include webs, zees, and tees for various t_w/t_f values.

Also, these charts may be used to determine the allowable buckling stress for local compression instability of conventionally stiffened plates which have been idealized into geometries similar to those shown in Figures C4.3.0-1 through C4.3.0-5. When this is done, care should be exercised that the dimensioning rules pertaining to formed and extruded shapes, as shown in Figure C4.2.2-8, are observed.

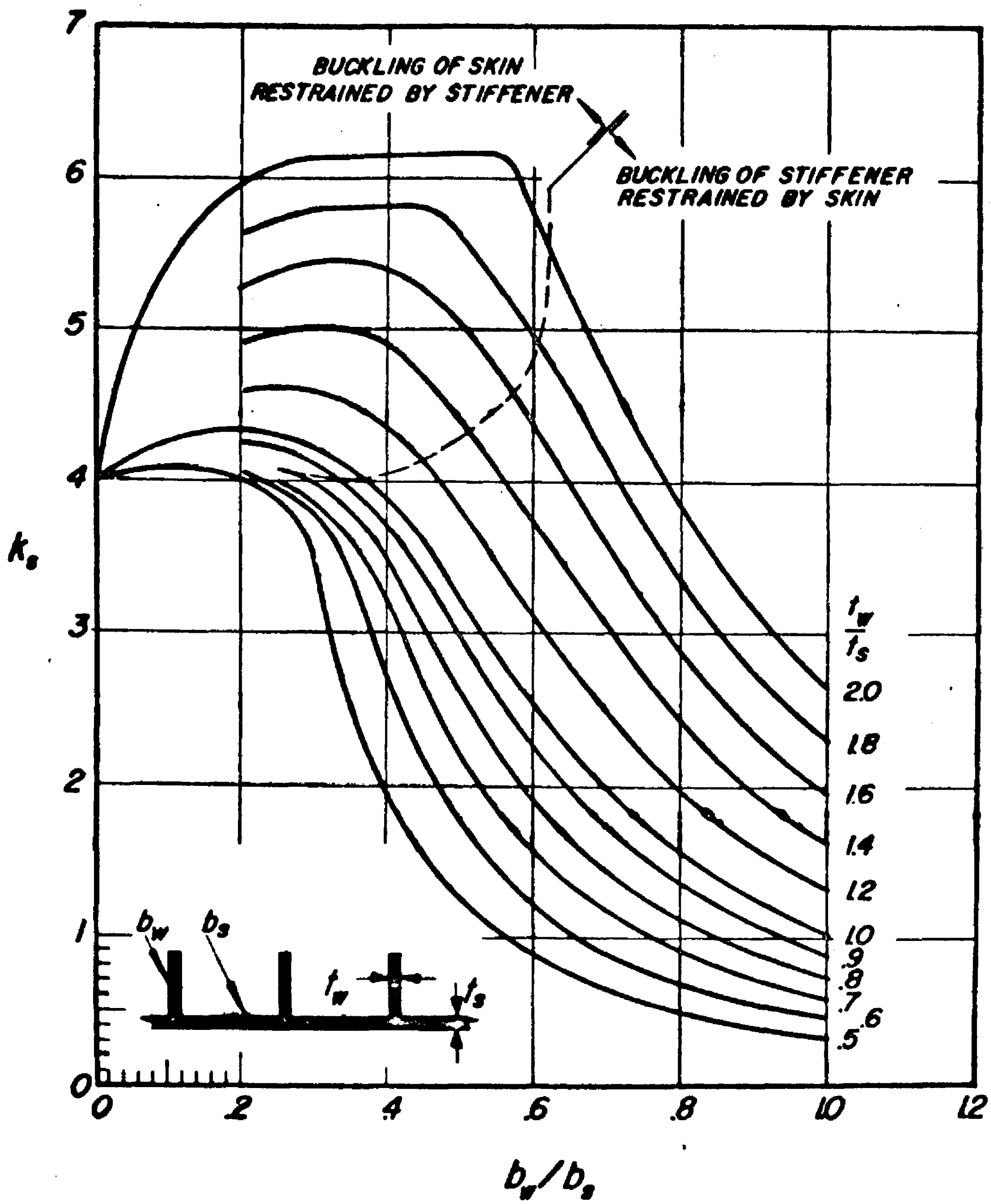

$0.5 < t_w/t_s < 2.0$

FIGURE C4.3.0-1. COMPRESSIVE-LOCAL-BUCKLING COEFFICIENTS FOR INFINITELY WIDE FLAT PLATES HAVING WEB-TYPE INTEGRAL STIFFENERS.

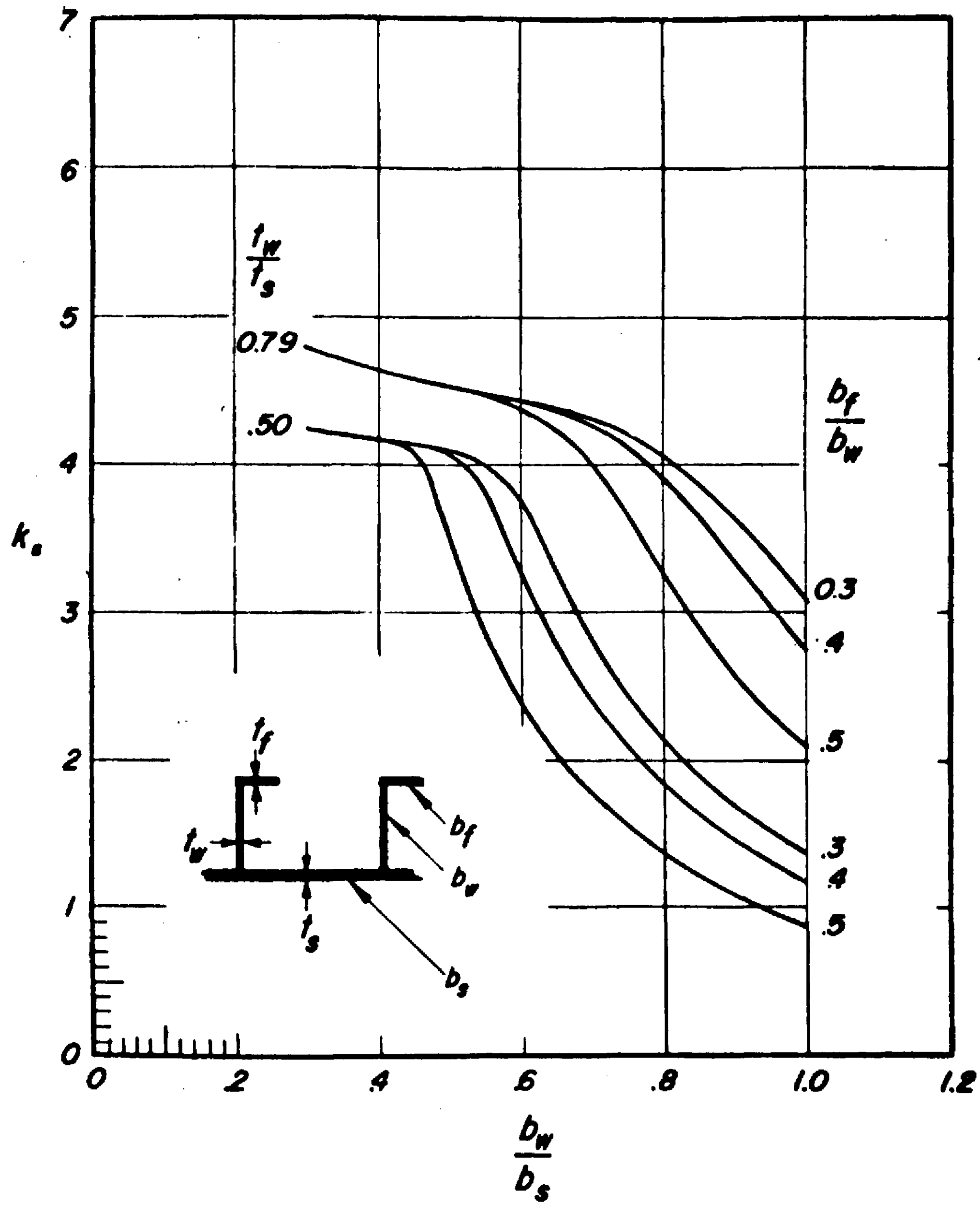

t_w/t_s = 0.50 and 0.79

FIGURE C4.3.0-2. COMPRESSIVE-LOCAL-BUCKLING COEFFICIENTS FOR INFINITELY WIDE FLAT PLATES HAVING Z-SECTION INTEGRAL STIFFENERS.

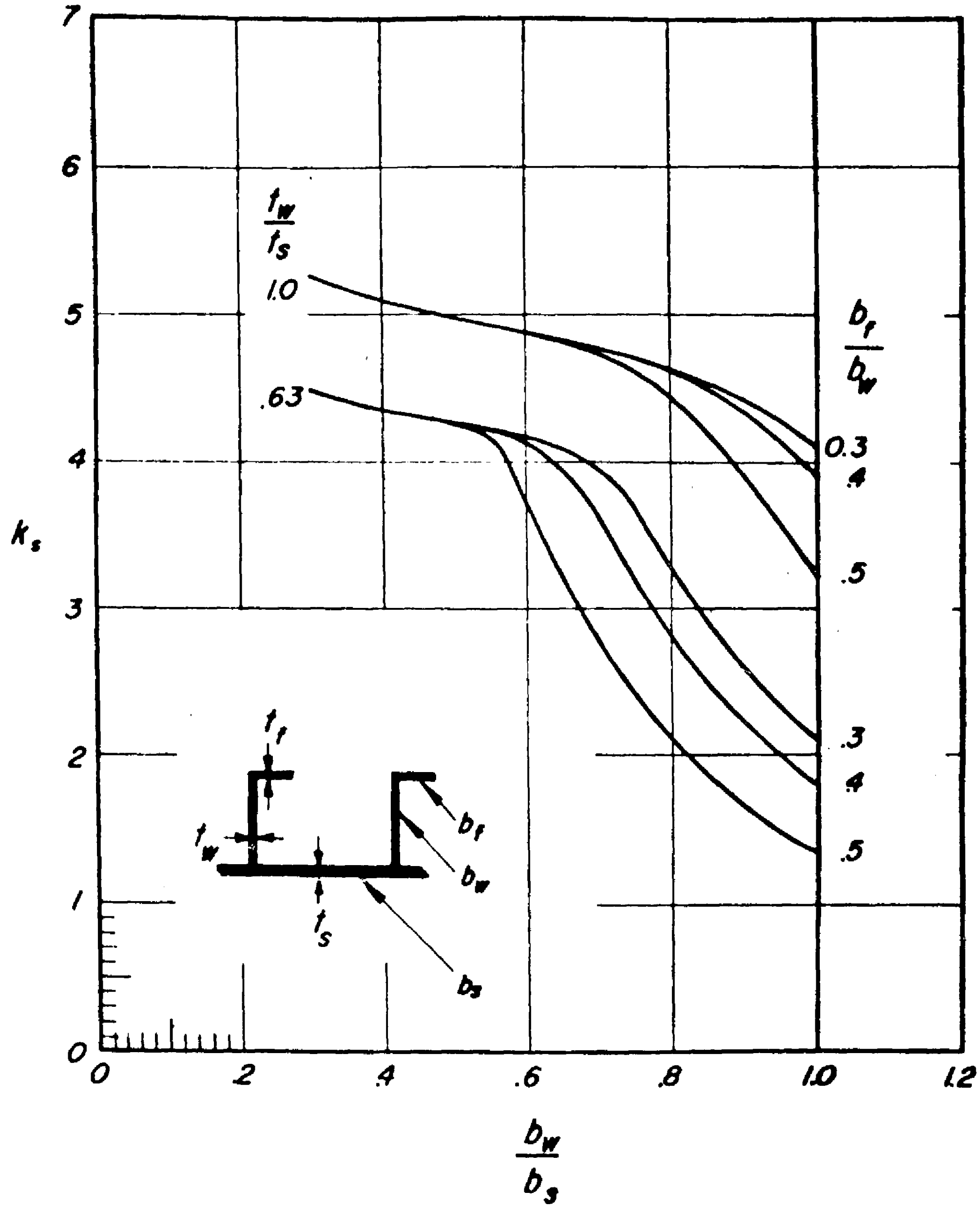

t_w/t_s = 0.63 and 1.0

FIGURE C4.3.0-3. COMPRESSIVE-LOCAL-BUCKLING COEFFICIENT FOR INFINITELY WIDE FLAT PLATES HAVING Z-SECTION INTEGRAL STIFFENERS.

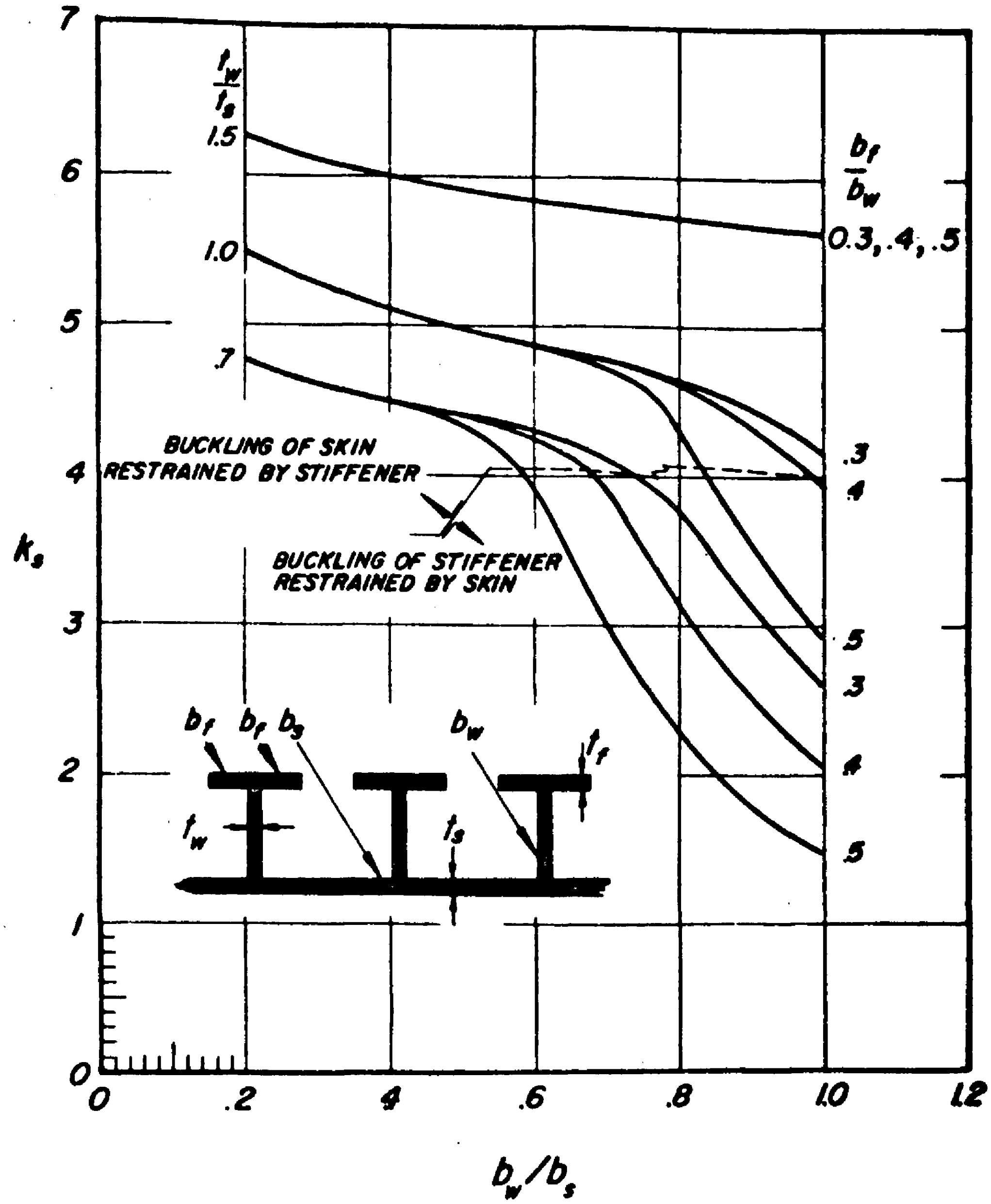

$t_w/t_f = 1.0$; $b_f/t_f > 10$; $b_w/b_s > 0.25$

FIGURE C4.3.0-4. COMPRESSIVE-LOCAL-BUCKLING COEFFICIENT FOR INFINITELY WIDE FLAT PLATES HAVING T-SECTION INTEGRAL STIFFENERS.

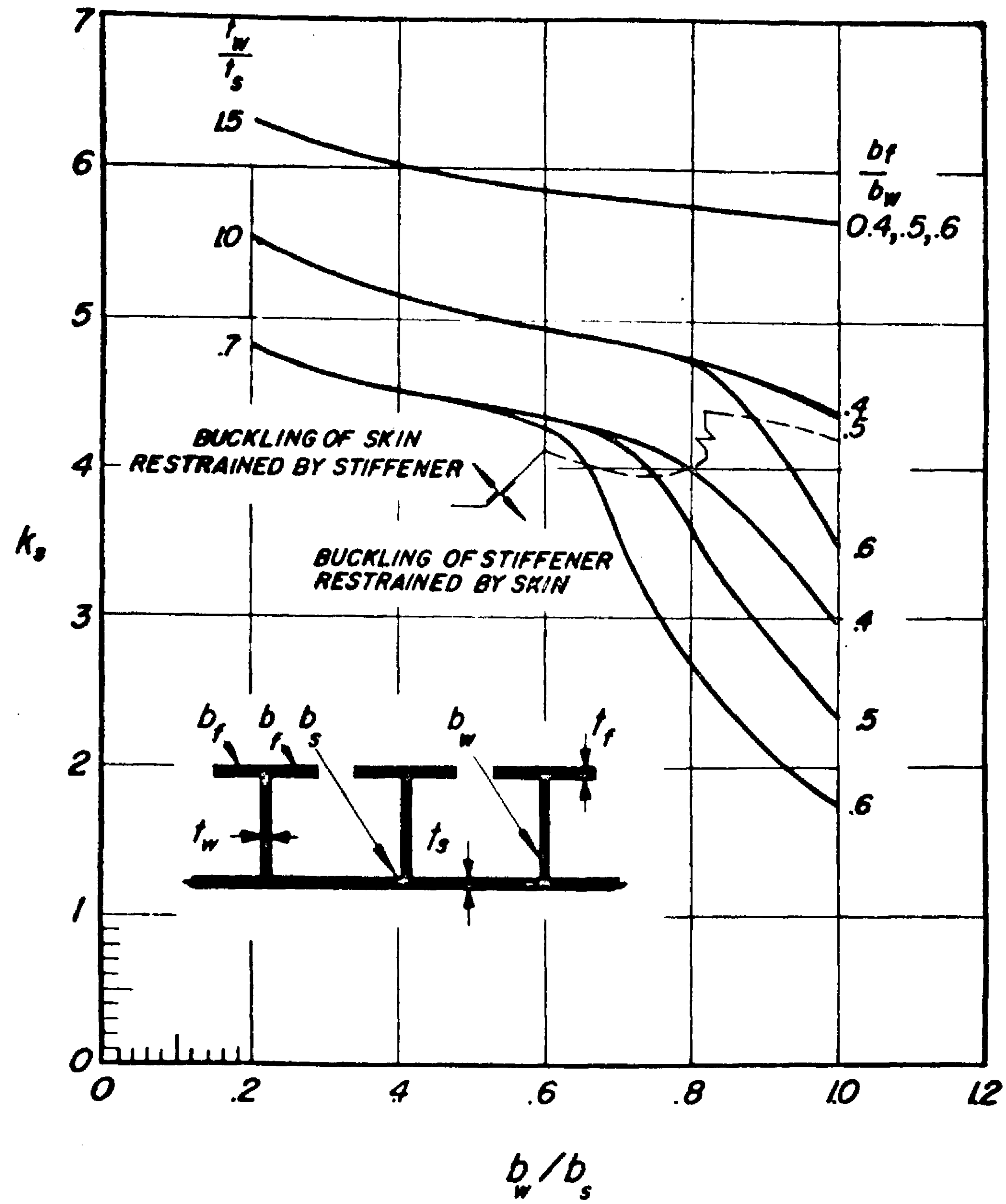

t_w/t_f = 0.7; b_f/t_f > 10; b_w/b_s > 0.25

FIGURE C4.3.0-5. COMPRESSION-LOCAL-BUCKLING COEFFICIENT FOR INFINITELY WIDE FLAT PLATES HAVING T-SECTION INTEGRAL STIFFENERS.

C4.4.0 Stiffened Flat Panels in Shear

Local shear instability methods of analysis for stiffened panels in shear are presented for panels stiffened either longitudinally or transversely. For shear buckling calculations, these two types of stiffened panels may be distinguished by considering panels with stiffeners parallel to the long side of the panel as longitudinally stiffened, and panels with stiffeners parallel to the short side of the panel as transversely stiffened. In instances where stiffened square panels are encountered, use of the analysis for transversely stiffened panels is recommended, to take advantage of the more extensive test data available.

The analysis that follows accounts for the local (no deflection of stiffeners) instability mode of failure only. The parameter $EI/b_s D$ is necessary for determining the criticality of the panel instability mode. At low values of $EI/b_s D$ the general (stiffeners deflect) mode is critical. As $EI/b_s D$ increases, the local mode becomes critical and yields a constant value of the shear buckling coefficient k_s regardless of further increases of $EI/b_s D$. Thus, in determining the flexural stiffness required in the stiffeners, it is this transition area of $EI/b_s D$ which is important since additional stiffener moment of inertia does nothing to increase allowable local plate buckling stress and less inertia induces general instability.

It is noted at this point that for similar bay geometries for the two different stiffening arrangements, equal local instability stresses will result. Local instability is a function of only the local geometry; whereas, general instability depends upon the orientation of the stiffeners with respect to the panel's long dimension.

The equation for local instability of the skin of a stiffened panel in shear is

$$F_{scr} = \eta \bar{\eta} \frac{k_s \pi^2 E_c}{12 (1-\nu^2)} \left(\frac{t_s}{b_s}\right)^2 , \qquad (26)$$

where k_s , the shear buckling coefficient, can be found by referring to Figure C2.1.5-14.

For longitudinally stiffened panels, using k_s determined above, enter Figure C4.4.0-1 and solve for a stiffener I required to prevent local skin buckling. The ratio between local buckling and general instability is as follows:

$$k_s \text{ (local)} = \frac{k_s \text{ (general)}}{(N+1)^2} , \qquad (27)$$

where N is the number of stiffeners. A stiffener I required to prevent general instability can be calculated in a similar manner using the ratio cited.

For transversely stiffened panels, a similar procedure to that given above can be used to calculate an I for the stiffeners required to resist local buckling; this is done by entering Figure C4.4.0-2 with a known k_s. The relationship between local buckling and general instability is

$$\frac{k_s \text{ (local)}}{b_s^2} = \frac{k_s \text{ (general)}}{a^2} . \qquad (28)$$

Using this relationship and the same figure, a required stiffener I can be calculated to prevent general instability.

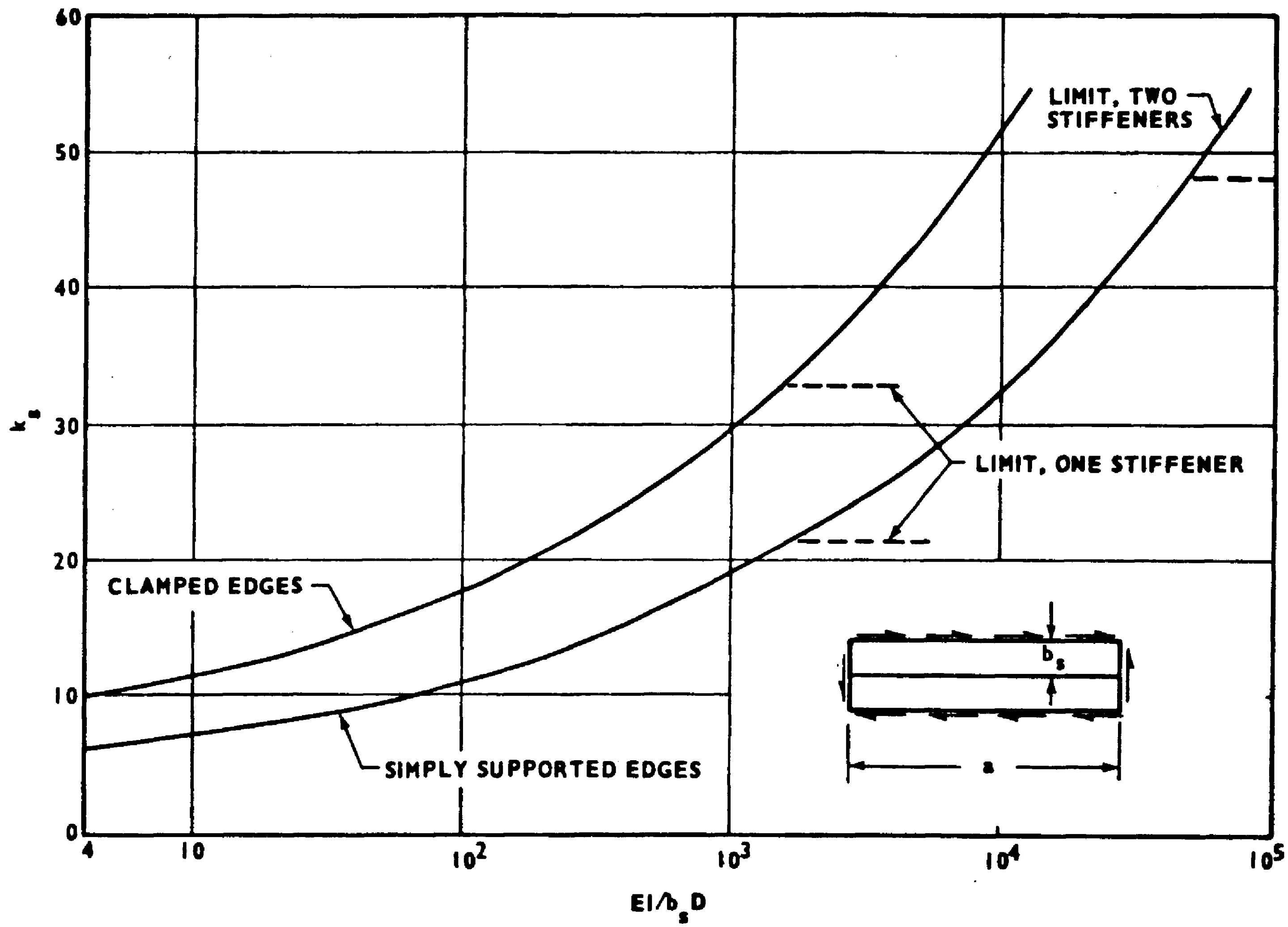

FIGURE C4.4.0-1. SHEAR BUCKLING COEFFICIENTS FOR LONG FLAT PLATES WITH LONGITUDINAL STIFFENERS.

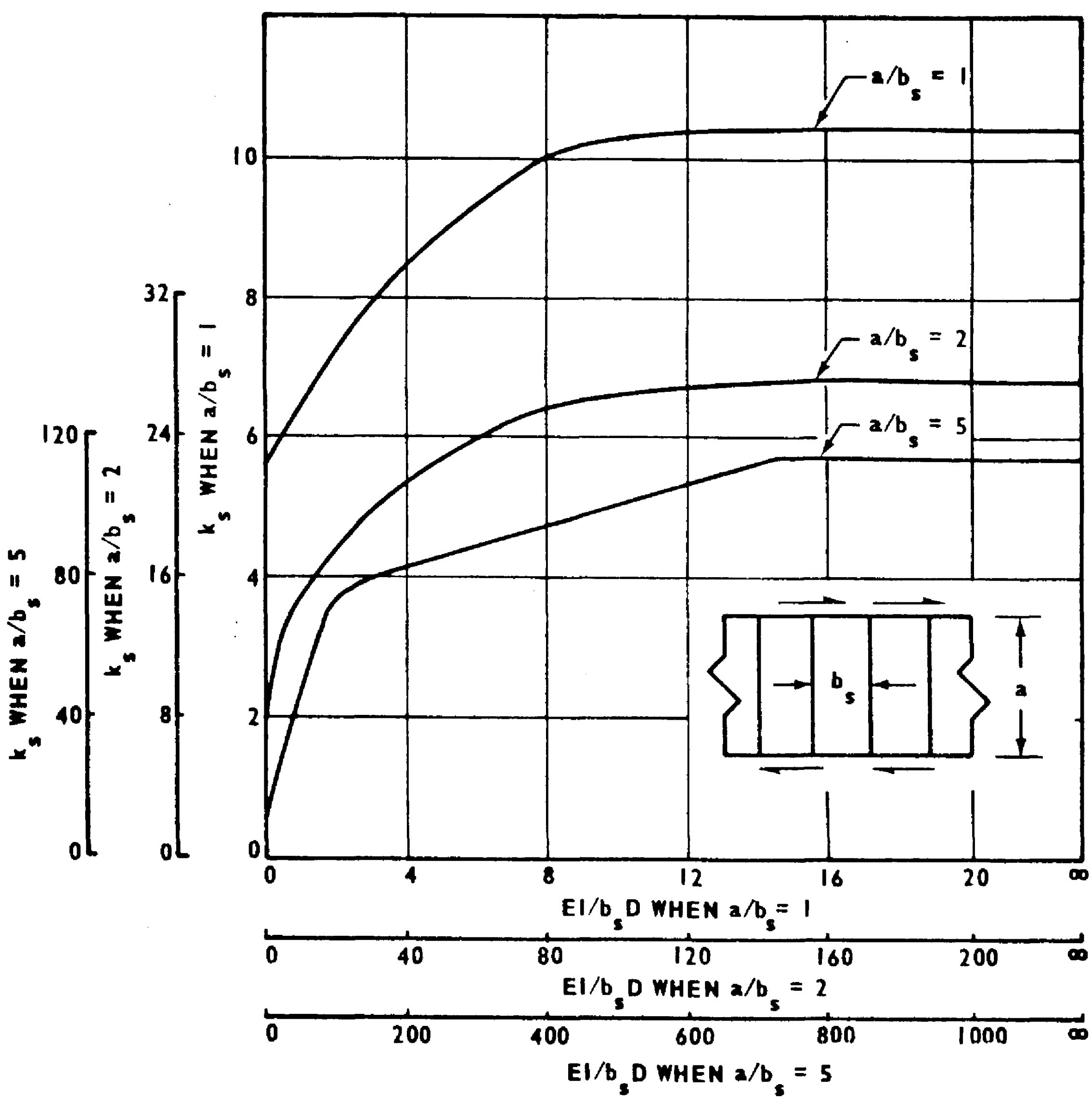

FIGURE C4.4.0-2. SHEAR BUCKLING COEFFICIENTS FOR LONG SIMPLY SUPPORTED FLAT PLATES WITH TRANSVERSE STIFFENERS.

The preceding relationships associate local and general modes of instability. It is then quite simple to discern which mode is critical to the structural integrity of the stiffened panel.

When F_{scr} is calculated, including plasticity and cladding correction factors if necessary, it should not exceed F_{co} given in Table C4.4.0.1, that is,

$$F_{scr} \leq F_{co} \qquad (29)$$

Table C4.4.0.1. Recommended Values for Shear Cutoff Stress

Material	Cutoff Stress (F_{co})
2024-T 2014-T 6061-T 7075-T	$0.61\ F_{cy}$
18-8 (1/2 H)*	$0.51\ F_{cy}$
(3/4 H)	$0.53\ F_{cy}$
(FH)	$0.53\ F_{cy}$
All other materials	$0.61\ F_{cy}$

* Cold-rolled, with grain, based on MIL-HDBK-5A properties.

C4.5.0 Flat Panel Stiffened with Corrugations †

C4.6.0 Stiffened Curved Panels ††

† to be supplied
†† to be supplied

References

1. NASA-Manned Spacecraft Center, Houston, Texas: Shell Analysis Manual.

2. Gerard, G.: Handbook of Structural Stability, Part V — Compressive Strength of Flat Stiffened Panels. NACA TN 3785, 1957.

3. Bruhn, E.: Analysis and Design of Flight Vehicle Structures. Tri-State Offset Company, Cincinnati, Ohio, 1965.

4. Argyris, J.: Flexure-Torsion Failure of Panels. Aircraft Engineering, June - July 1954.

5. North American Aviation, Inc.: Structures Manual.

Bibliography

Argyris, J. and Dunne, P.: Structural Principles and Data, Part 2, Structural Analysis. Handbook of Aero., No. 1, Fourth Edition, Sir Isaac Pitman & Co., Ltd. London, 1952.

Becker, H.: Handbook of Structural Stability, Part II — Buckling of Composite Elements. NACA TN 3782, 1957.

Gerard, G. and Becker, H.: Handbook of Structural Stability, Part I — Buckling of Flat Plates. NACA TN 3781, 1957.

Gerard, G.: Handbook of Structural Stability, Part IV — Failure of Plates and Composite Elements. NACA TN 3784, 1957.

Lockheed — Missiles and Space Division: Structural Methods Handbook.

Semonian, J. and Peterson, J.: An Analysis of the Stability and Ultimate Compressive Strength of Short Sheet-Stringer Panels with Special Reference to the Influence of Riveted Connection Between Sheet and Stringer. NACA TN 3431, 1955.

APPROVAL

ASTRONAUTIC STRUCTURES MANUAL
VOLUME II

The information in this report has been reviewed for security classification. Review of any information concerning Department of Defense or Atomic Energy Commission programs has been made by the MSFC Security Classification Officer. This report, in its entirety, has been determined to be unclassified.

This document has also been reviewed and approved for technical accuracy.

A. A. McCOOL
Director, Structures and Propulsion Laboratory

☆U.S. GOVERNMENT PRINTING OFFICE 1977—740-049/189 REGION NO. 4